Characterization of Droplets and Vapor Concentration Distributions in Split-Injection Diesel Sprays by Processing UV and Visible Images*

Yuyin ZHANG**, Keiya NISHIDA** and Takuo YOSHIZAKI***

Recent experimental studies have shown that with split injection strategy, the soot and NO_x emissions from a diesel engine can be reduced significantly in comparison with a conventional non-split injection. To understand the mechanism of emissions reduction, it is essential to clarify the process of mixture formation in the diesel spray. For characterizing the droplets and vapor concentration distributions inside a fuel spray, a dual-wavelength laser absorption-scattering technique (LAS) was developed by using the 2nd harmonic (532 nm) and the 4th harmonic (266 nm) of an Nd : YAG laser and using dimethylnaphthalene as a test fuel. By applying the ultraviolet-visible LAS imaging technique, the distributions of droplets and vapor concentrations in the spray, which was injected into a high-temperature and high-pressure nitrogen ambient in a constant volume vessel by a common-rail diesel injection system, were measured and quantitatively analyzed. The effect of injection mass ratio of double-pulse injections on distributions of equivalence ratios of vapor and droplets in the sprays was examined.

Key Words: Diesel Engine, Laser-based Diagnostics, Fuel Injection, Evaporation

1. Introduction

The experimental results[1-3] have shown that NOx and particulate emissions of a DI diesel engine can be markedly reduced by use of appropriate split-injection schemes. It is clear that the injection mass ratios and the dwell(s) between injections are critical to the engine emission performances. However, the characteristics of mixture formation inside a split-injection diesel spray, which dominates combustion and NOx/particulate formation of a diesel engine, remains unexplained[4].

As vapor and liquid droplets exist concurrently in the diesel spray, the quantitative measurement becomes complicated. Some researchers have proposed valuable approaches in attempting such measurements, including laser induced Exciplex fluorescence (LIEF)[5] and infrared extinction[6]. In the recent decade, Suzuki et al.[7] and Zhang et al.[8-11] proposed an optical diagnostic based on ultraviolet-visible laser absorption-scattering (LAS) to detect the vapor concentration and droplets density inside a fuel spray. As the LAS technique can provide quantitative concentration information of both vapor and droplets, the signal-to-noise ratio is high, and not easily affected by oxygen quenching which is often encountered in LIEF, or by heat radiation from heater and any hot point around frequently encountered in infrared extinction, it is considered as a promising approach.

In this paper, the measurement principle of the ultraviolet-visible LAS technique was, at first, briefly introduced. Then, an uncertainty verification on vapor measurement by the LAS technique was performed through measurements on a series of completely-evaporated diesel sprays. And, finally, the

* Received 20th June, 2002 (No. 02-4193)

** Dept. of Mechanical System Engineering, University of Hiroshima, 1-4-1 Kagamiyama, Higashi-Hiroshima 739-8527, Japan. E-mail : nishida@mec.hiroshima-u.ac.jp

*** Dept. of Mechanical Engineering, Nippon Institute of Technology, 4-1 Gakuendai, Miyashiro-cho, Saitama-gun, Saitama 345-8501, Japan

characteristics of split-injection diesel spray impinging perpendicularly on a flat-wall in a high-temperature and high-pressure nitrogen atmosphere were investigated by use of the LAS technique. The effects of injection mass ratio of double-pulse injection on distributions of fuel vapor and droplets in the diesel sprays were quantitatively examined. The experimental conditions were set referring to those of an actual DI diesel engine at the start of injection. For split-injections, the injection mass ratio of the first pulse varies from 25% to 75% with a fixed dwell of 1.0ms and fixed injection quantity of 20.5mg/cycle/hole.

2. Laser Absorption-Scattering (LAS) Technique

2.1 Principle

The ultraviolet-visible LAS technique consists of two measurements: a transmission measurement of visible light to detect the optical thickness of droplets at the transparent wavelength and a transmission measurement of ultraviolet light to determine the joint optical thickness of vapor and droplets at the absorbing wavelength. When passing through a fuel spray, the total light extinction at this absorbing wavelength is a result of droplets scattering, droplets absorption, and vapor absorption. The optical thickness of droplets at the two wavelengths is very close to each other in many cases, which we will explain later in this section. Therefore, the optical thickness of vapor can result from removing the droplets optical thickness at the transparent wavelength from the joint optical thickness of vapor and droplets at the absorbing wavelength. The vapor concentration will be then yielded through utilizing an onion-peeling model for axisymmetric sprays, and the droplets density can be attained from the optical thickness of droplets when the number density and size distribution of droplets are available. Detailed discussions of the principle can be found in our previous papers[8]. A brief introduction of the principle follows.

The intensity $I_t(\lambda)$ of laser light transmitted through a mixture of vapor and droplets is related to the intensity $I_0(\lambda)$ of the incident light by the Bouguer-Lambert- Beer's law as follows:

$$\log\left(\frac{I_0}{I_t}\right)_\lambda = \int_0^L \varepsilon(\lambda)\cdot C_v dx + \int_0^L K_{ext}(\lambda) dx \qquad (1)$$

where λ is the wavelength of incident light, $\varepsilon(\lambda)$ is the absorption coefficient of fuel vapor, C_v is the vapor concentration, L is the optical path length, and K_{ext} is the extinction coefficient for a cloud of droplets. K_{ext} is defined as:

$$K_{ext}(\lambda) = -\frac{\pi}{4} C_n \int_0^\infty Q_{ext}(\lambda)\cdot N(D)\cdot D^2 dD \qquad (2)$$

where C_n is the number density of droplets, $Q_{ext}(\lambda)$ is the extinction efficiency of droplets at wavelength λ, D is the droplets diameter, and $N(D)$ is the droplets size distribution function.

The first term on the right hand side of Eq.(1) represents the light extinction due to vapor only and the second term is the light extinction due to droplets only. The latter includes light scattering and absorption. In other words, $Q_{ext}(\lambda)$ in Eq. (2) is the sum of scattering efficiency $Q_{sca}(\lambda)$ and absorption efficiency $Q_{abs}(\lambda)$.

When the incident light includes two wavelengths, i.e. the absorbing wavelength λ_A and the non-absorbing wavelength λ_T, there will be:

$$\log\left(\frac{I_0}{I_t}\right)_{\lambda_A} = \varepsilon(\lambda_A)\cdot \overline{C_v}\cdot L + \overline{K_{ext}(\lambda_A)}\cdot L \qquad (3)$$

$$\log\left(\frac{I_0}{I_t}\right)_{\lambda_T} = \overline{K_{ext}(\lambda_T)}\cdot L \qquad (4)$$

where the line-of-sight averaged terms are indicated by an overbar. From Eqs. (3) and (4), the line-of-sight averaged vapor concentration can be derived as follow:

$$\overline{C_v} = \frac{1}{\varepsilon(\lambda_A)\cdot L}\left[\log(I_0/I_t)_{\lambda_A} - R\cdot\log(I_0/I_t)_{\lambda_T}\right] \qquad (5)$$

where R is the ratio of the drop optical thickness at the two wavelengths and defined as:

$$R = \left[\frac{\log(I_0/I_t)_{\lambda_A}}{\log(I_0/I_t)_{\lambda_T}}\right]_{droplets} = \frac{\int_0^\infty [Q_{sca}(\lambda_A)+Q_{abs}(\lambda_A)]N(D)\cdot D^2 dD}{\int_0^\infty Q_{sca}(\lambda_T)\cdot N(D)\cdot D^2 dD} \qquad (6)$$

It is clear from Eq.(5) that the vapor concentration is obtained if extinction measurements at two wavelengths, i.e. $\log(I_0/I_t)_{\lambda A}$ and $\log(I_0/I_t)_{\lambda T}$, are implemented and, R and $\varepsilon(\lambda_A)$ is known.

Equation (6) indicates that the droplets absorption at λ_A contributes to the extinction efficiency. In addition, to obtain R, the size distribution of droplets is required. However, in many cases, R is approximately 1, as the droplets extinction efficiencies at the two wavelengths approach each other in those cases. The investigation of Drallmeier et al.[12] shows that for sprays with area

Table 1 Physical properties of candidate liquid fuels

Fuel	Diesel JIS #2	n-Tri-decane $C_{13}H_{28}$	n-Tetra-decane $C_{14}H_{30}$	n-Penta-decane $C_{15}H_{32}$	n-Cetane $C_{16}H_{32}$	1,3-Dimethyl-naphthalene $C_{10}H_6(CH_3)_2$	α-Methyl-naphthalene $C_{10}H_7(CH_3)$
Boiling point ℃ (1 atm.)	273*	235	253.7	270.6	287.0	265.2	244.7
Density kg/m^3 (20°C, 1 atm.)	830	756	760	770	780	1018	1020
Kinetic viscosity mm^2/s (20°C, 1 atm.)	3.86	2.47	3.04	3.73	4.52	3.95	2.58

*Volumetric Average Boiling Point

mean diameter D_{20} greater than 20 μm, there appears $R\approx1$. D_{20} is defined as:

$$D_{20}=\left[\frac{\sum N(D)\cdot D^2 dD}{\sum N(D)dD}\right]^{\frac{1}{2}} \tag{7}$$

For the case of the ultraviolet-visible LAS technique in this work, it is clarified by Zhang et al.[9] that the optical thickness of droplets in a non-evaporating diesel spray at the two wavelengths is very close to each other in the region apart from the spray axis. In the vicinity of the spray axis, the optical thickness at λ=266nm is a little greater than that at λ=532nm. In other words, the ratio of the droplets optical thickness at the two wavelengths approaches 1 except for in the region very close to the spray axis, where the droplets is considerably dense. Another significance of this is seen in the implication that knowledge of the size distribution is not vital if the droplets cluster is not extremely dense. Practically, even in the droplet-dense region, for an evaporating diesel spray, the vapor optical thickness dominates the total extinction, reducing the impact of the difference of droplets optical thickness at the two wavelengths[9].

The other terms which is critical on calculating the vapor concentration by Eq. (5) are the absorption coefficient of fuel vapor $\varepsilon(\lambda_A)$, which can be examined by an optical spectrometer with a high-pressure and high-temperature absorption cell, and the optical thickness at the two wavelengths $\log(I_0/I_t)_{\lambda A}$ and $\log(I_0/I_t)_{\lambda T}$, which can be attained by using a CCD-camera imaging system with dual wavelength laser light.

On the other hand, the line-of-sight average droplets density in the spray can be related, based on the light scattering theory[13, 14], to the optical thickness at the non-absorbing wavelength λ_T, as shown in the following equation:

$$\overline{C_d}=2.303\cdot\frac{2}{3L}\cdot\rho_f\cdot\frac{D_{32}}{R_k Q_m}\cdot\log\left(\frac{I_0}{I_t}\right)_{\lambda_T} \tag{8}$$

where ρ_f is the liquid fuel density, D_{32} is known as Sauter mean diameter, R_k is the correction factor related to the detecting half-angle of the optical system and size parameter of droplets, and Q_m is the mean extinction efficiency for a poly-dispersed particle cloud, respectively. The mean extinction efficiency Q_m approaches a constant of 2 as the droplet size becomes much larger than the wavelength. The Sauter mean diameter D_{32} can be determined experimentally by the Fraunhofer diffraction technique or be approximated using summation of the optical thickness of the fuel droplets in the entire spray plume[14]:

$$D_{32}=\frac{0.63\,R_k\cdot Q_{ext}\cdot M_f}{\rho_f\sum_S\left[\log\left(\frac{I_0}{I_t}\right)_{\lambda_T}\cdot\Delta S\right]} \tag{9}$$

where ΔS is the unit projection area in the spray and M_f is the total mass of liquid fuel within the spray.

Thus, it can be seen from the above that two transmission measurements are necessary to detect the vapor concentration and droplets density when the absorption coefficients of the test fuel is available. A transmission measurement of visible light determines the optical thickness of droplets and thus droplets density. A transmission measurement of ultraviolet light together with the transmission measurement of visible light determines the optical thickness of vapor, which is in turn related to the vapor concentration.

2.2 Investigation of Test Fuel

In order to detect the fuel distribution in a diesel spray using the ultraviolet-visible LAS technique, a test fuel with following physical and optical properties should be available:

- having physical properties including boiling point, viscosity and evaporation rate are close to those of the diesel fuel;
- being a strong absorber of ultraviolet at λ=266nm and non-absorbing at λ=532nm;
- having no or weak temperature-dependence of absorption coefficients for measuring sprays injected into a high-temperature atmosphere.

According to the above-mentioned criteria, screening of the test fuel was conducted, which was described in our previous paper[8].

Some liquid fuels, which have physical properties close to those of the diesel fuel, were selected as candidate test fuels (Table 1). The measurements of absorption spectra of the fuels were performed in our previous work[8] using an ultraviolet-visible spectrophotometer (Shimadzu UV-3000). Figure. 1 shows the measurement results of the spectra at normal atmosphere and room temperature. It is not difficult to see that all of the fuels absorb ultraviolet and do not absorb visible light. 1,3-Dimethyl-naphthalene (DMN) is the strongest ultraviolet absorber in the group, and the α-methylnaphthalene (α-MN) is the second. Therefore, DMN was employed as the test fuel in this work. Beside the above-mentioned properties suitable for the LAS imaging system, DMN has, of course, more properties superior to the other fuels, such as a plainer temperature-dependence of absorption coefficients.

Molar absorption coefficients of DMN vapor at λ=266nm at elevated temperatures and pressures are shown in Fig 2, in comparison to those of α-MN at λ=280nm, which was used in the previous work[7]. The absorption coefficients of DMN were measured by an optical spectrometer (S2000, Ocean Optics) at a high-temperature and high-pressure absorption cell. The data indicate that molar absorption coefficients of

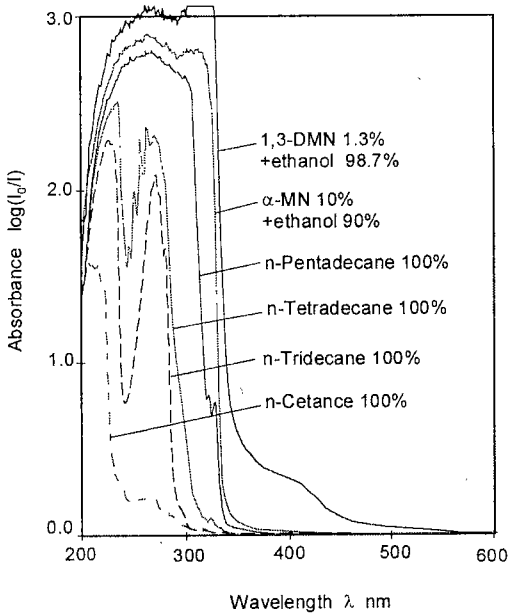

Fig. 1 Absorption spectra of test fuels in liquid phase[8] (T_a=298K, P_a=0.1MPa, L=10mm). Ethanol was used as the solvent to dilute 1,3-DMN and α-MN to avoid exceeding the measurement range of the instrument.

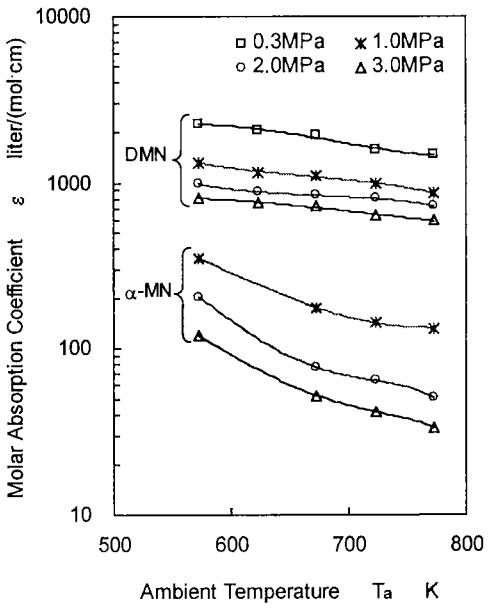

Fig. 2 Molar absorption coefficients of DMN vapor at λ=266nm and α-MN vapor at λ=280nm

DMN at λ=266nm depend on temperature and pressure. Compared to those of α-MN at λ=280nm, however, the temperature-dependence of absorption coefficients of DMN is much smaller. The importance of this is that the accuracy of vapor measurement using DMN will not be greatly affected by the temperature distribution in the fuel spray, when the local temperature is unknown. Moreover, the magnitude of molar absorption coefficients of DMN is greater, which can improve the resolution of the fuel vapor measurement.

So far, we have seen that the properties of DMN have covered all the requirements using the UV-visible LAS technique to determine the vapor concentration and droplets density in a diesel spray.

3. Experimental Apparatus and Conditions

We have shown that it is feasible to simultaneously obtain the quantitative information of the distributions of fuel vapor and droplets in a spray using the ultraviolet-visible LAS technique, that is, using the fourth harmonic and the second harmonic of a pulsed Nd:YAG laser as the light source and DMN as the test fuel.

A schematic of the optical arrangement of the ultraviolet-visible LAS imaging system and the spray injection system was shown in Fig. 3. A coaxial laser beam consisting of the second harmonic and the fourth harmonic of an Nd:YAG laser (Continuum Co.,

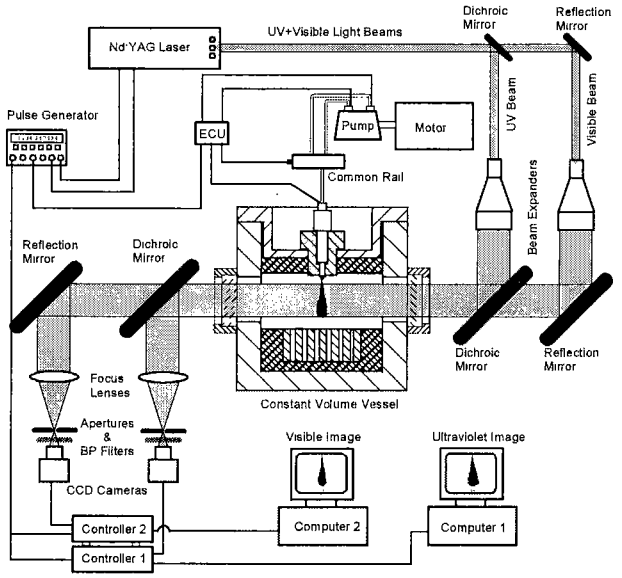

Fig. 3 A schematic of UV-visible laser absorption-scattering imaging for measurements of diesel spray

NY61-10, Pulse width: 6ns, Max. power: 300mJ for 532nm and 60mJ for 266nm) was separated into two, i.e., an ultraviolet beam (266nm) and a visible beam (532nm), by a dichroic mirror. The two beams were then expanded to ϕ100mm by a visible beam expander and an ultraviolet beam expander respectively. A reflection mirror and a dichroic mirror made the two expanded beams coaxial again and directed the coaxial one to the fuel spray injected into a constant volume vessel. After being attenuated due to absorption and/or scattering of the fuel vapor and droplets, the beam were re-separated into two, a visible one and an ultraviolet one. Then, a pair of collimating lens (ϕ150mm, f=500mm) focused the two beams into the respective CCD cameras (Photometrics Star I, 384×576 pixels, 12 bit grayscale). Spectral filters and apertures before the CCD cameras cut off the optical noises beyond the incident wavelength and scattered light beyond the optical half angle, respectively. The image acquisition and arithmetic processing was carried out by an IPLab (Spectrum Signal Analytics Corporation) image analysis system.

A common-rail diesel injection system was used to inject an fuel spray into a high-temperature and high-pressure constant volume vessel filled with nitrogen gas. The laser pulse was triggered by the injection pulse from ECU of the common-rail injection system through the Q-switch of the Nd:YAG laser. A pulse generator synchronized the Nd:YAG laser, the CCD cameras, and the injection system. A diesel injector with one single orifice nozzle, which was specially built for the test, was employed. The diameter and length of the orifice keeps the same as those used in a commercial engine, but the number of orifices was changed from original 4 to 1.

Table 2 Experimental conditions

Ambient gas	Nitrogen
Temperature T_a	833 K
Pressure P_a	4.0 MPa
Density ρ_a	16.2 kg/m^3
Fuel	Dimethylnaphthalene
Fuel Injection system	Common Rail Type
Injection pressure P_{inj}	90 MPa
Number of orifice	1
Diameter of orifice d_n	0.21 mm
Length-to-diameter	3.8:1
Injection quantity M_f	20.5mg/cycle
Impingement flat-wall	Steel
Imping. distance L_w	31 mm
Imping. angle	90°

The experimental conditions are listed in Table 2. Two experiments were performed in the present paper. One was done for verifying the vapor measurement accuracy. Therefore, the injection durations were set rather short (0.22~1.00ms), and the mass of fuel injected were among 2.1~10.3mg/cycle, allowing the fuel evaporated completely before the plume of the spray exceeded the scope of the observation window when it was shot.

Another experiment was done for determining both the vapor concentration and droplets density in split-injection diesel sprays at the start of the second injection and after the start of the second injection. The injection ratios and the dwell between injections

Table 3 Fuel injection schemes

Scheme	Inj. ratio (1st pulse)	Dwell (ms)	Inj. ratio (2nd pulse)
D75-1.0-25	75%	1.0	25%
D50-1.0-50	50%	1.0	50%
D25-1.0-75	25%	1.0	75%

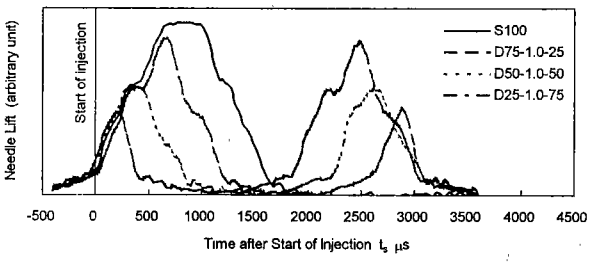

Fig. 4 Needle lift of split injections

were given in Table 3. The needle lifts of the different split-injection schemes are shown in Fig. 4. The injection mass ratio of the first pulse varied from 75% to 25%. For all of split-injection cases, the total mass of fuel injected was set at 20.5mg, which was coincided with the mass of fuel injected by one of the four orifices of an actual diesel engine injector at the full load of the engine. The injection pressure, the ambient temperature and the ambient pressure were also set referring to those of the actual engine.

4. Results and Discussion

4.1 Verification of Fuel Vapor Measurement

An error analysis of vapor measurement in a fuel spray via the LAS technique has been implemented in the reference[4]. It has been shown that under the assumption of axisymmetric fuel spray, an error of about 5% in the vapor measurement is likely incurred in the region where the fuel vapor dominates, but it increases up to about 20% in the region where the vapor optical thickness is small. For verifying the vapor measurement by the LAS technique, a series of measurements were carried out.

Diesel sprays impinging on a flat wall with different injection quantity were imaged using the LAS technique. By the deconvolution method using the onion-peeling model[4, 10, 15], the vapor mass can be obtained from the spray images. The laser shot timings were varied to observe the variation of the vapor mass and droplets. When the vapor mass ceases to increase with time and no droplets can be detected by the visible image, we think that the droplets have evaporated completely then. The results are shown in Fig. 5. The measurement result by the LAS technique was regularly a little greater than the mass of fuel injected, but generally, the mass of the fuel vapor measured by the LAS technique is coincided with the fuel mass injected. It is proved that the vapor measurement by the LAS technique is reliable.

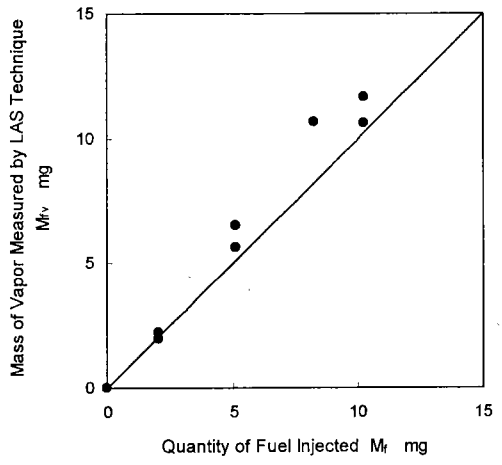

Fig. 5 A comparison of vapor mass measured by LAS technique to quantity of fuel injected (T_a=833K, P_a=4.0MPa, P_{inj}=90MPa, d_n=0.21mm, L_w=31mm)

4.2 Effect of Injection Mass Ratio on Fuel Distributions

The above comparisons of fuel vapor measurements by the LAS technique and mass of fuel injected give confidence in the fuel distribution characterization capabilities of the ultraviolet-visible LAS technique. In order to know the mechanism of mixture formation in split-injection diesel sprays, a set of injection schemes was measured and quantitatively analyzed by the LAS technique. The experimental conditions and injection parameters were given in Tables 2 and 3, respectively, in the previous section.

Figures 6 and 7 shows the contours of equivalence ratios of vapor and droplets in the sprays at the start of the second injection and at about 0.5ms succeeding to the start of the second injection, respectively. It is easily seen that most of the fuel in the sprays has evaporated at the start of the second injection due to an adequately long dwell (1.0ms) between injections. Moreover, the fuel vapor exists mainly in two regions: the non-impinged part of the spray which is dominated by the rich vapor-gas mixture and the impinged part of the spray which is occupied by the lean mixture. Also, in the impinged part, a richer mixture region near the spray tip can be observed in all the cases. It is believed that the wall jet vortex in the front of a spray, which was often observed in non-evaporating impingement diesel sprays [16-17], results in this kind of phenomenon.

On the other hand, the data of the sprays at about 0.5ms succeeding to the start of the second injection (see Fig. 7) indicate that the rich mixture in the non-impinged part which is generated by the first injection pulse has been driven to the outer of the spray, and the distribution of the equivalence ratio of vapor around the spray axis tends towards more uniform. We call this phenomenon "the turbulent effect" by the subsequent injection.

For ascertaining this outward-spreading of the vapor phase due to the subsequent injection, a comparison was made in Fig. 8 of the vapor

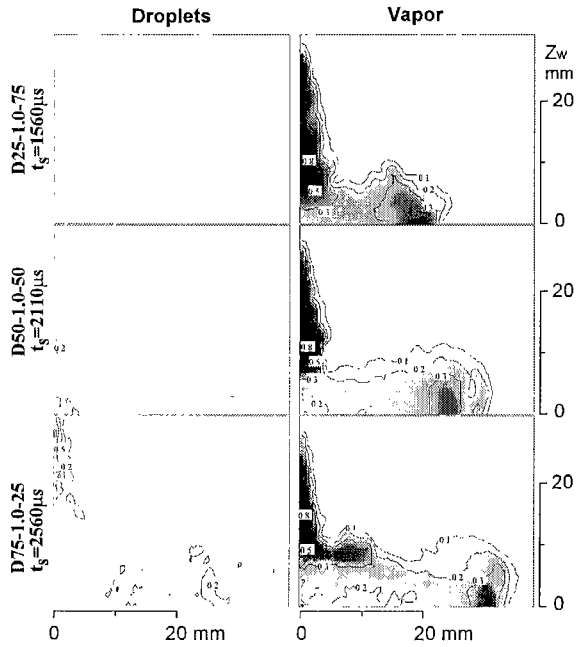

Fig. 6 Equivalence ratio distributions in split injection diesel sprays (at the start of the second injection)

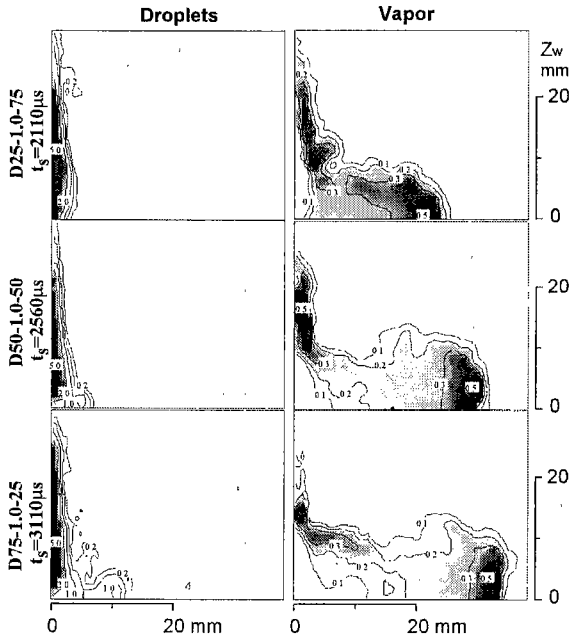

Fig. 7 Equivalence ratio distributions in split injection diesel sprays (at 0.5ms after the 2nd injection starts)

distribution between a split injection (D25-1.0-75) and a single injection spray (S25) with the same injection quantity as injected in the first pulse of D25-1.0-75. As seen in Fig. 8 , for the case of the single injection spray (on the left hand side), the vapor phase in the impinged part extends forwards, but that in the non-impinged part spreads scarcely in direction away from the spray axis and the rich mixture in the non-impinged part remains as time elapses. In contrast, in the split injection spray (on the right hand side), the rich mixture formed by the first injection pulse disappears and the vapor region in the non-impinged part extends outwards from the spray axis after the subsequent injection starts. This fact evidences that "the turbulent effect" of the subsequent injection does exist.

The radial distributions of equivalence ratios in the above sprays at axial distances of Z_w=12, 8, and 2mm from the impingement wall are given in Fig. 9 (at the start of the second injection) and in Fig. 10 (at 0.5ms after the start of the second injection). The general trend is that for all the three split injection schemes, the vapor distributions in the non-impinged part at about 0.5ms after the second injection starts are more uniform than those before the second injection start. Additionally, it is clear that the vapor phase moves in the direction away from the spray axis as the high-concentration vapor in the non-impinged part of the spray injected in the first pulse disappears, and the vapor concentration in the vicinity of the spray axis becomes lower and more uniform after the second injection starts. These imply that the subsequent injection plays an important role in the fuel-air mixing by entraining more air into the spray. Thus, it is reasonable to believe that the turbulent effect due to the subsequent injection in a split-injection may have potential to enhance the combustion in the later stage and the re-burning of particulate generated in the earlier combustion stage in the diesel engine, reducing the particulate emission.

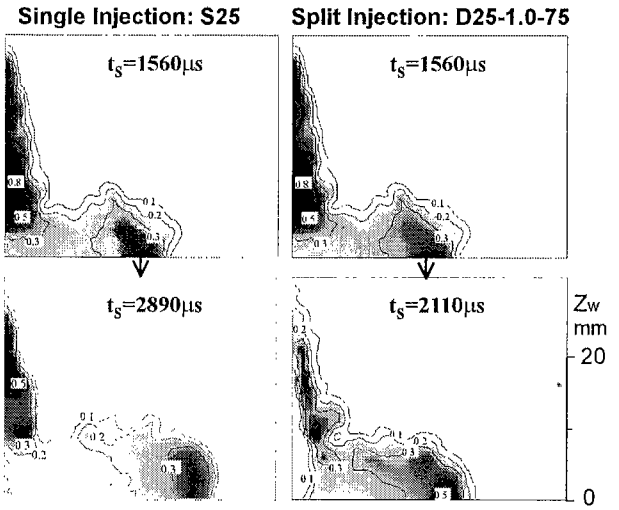

(Left) (Right)

Fig. 8 Difference in vapor distribution between split injection spray and single injection with the same injection quantity

5. Conclusions

By applying the ultraviolet-visible laser absorption-scattering (LAS) technique, the characteristics including the fuel distribution in the split-injection diesel sprays impinging on a flat-wall were investigated. The effect of an injection mass ratio on spray characteristics was examined. The main conclusions are as follows.

The mass of the fuel vapor measured by the LAS technique is generally coincided with the fuel mass injected, indicating the vapor measurement by the LAS technique is considerably reliable.

The injection mass ratio has a marked effect on the fuel distributions in the split diesel spray. After the start of the subsequent injection pulse, the rich mixture in the non-impinged part of the spray which is generated by the first injection pulse is driven to the outer of the spray, and the distribution of the equivalence ratio of vapor in the non-impinged part tends towards more uniform and leaner. In other words, the subsequent injection of a split injection scheme has a turbulent effect on the fuel-air mixing and the turbulent effect of the subsequent injection can enhance the fuel-air mixing in the diesel spray.

Acknowledgements

This research was supported in part by Denso Co.,

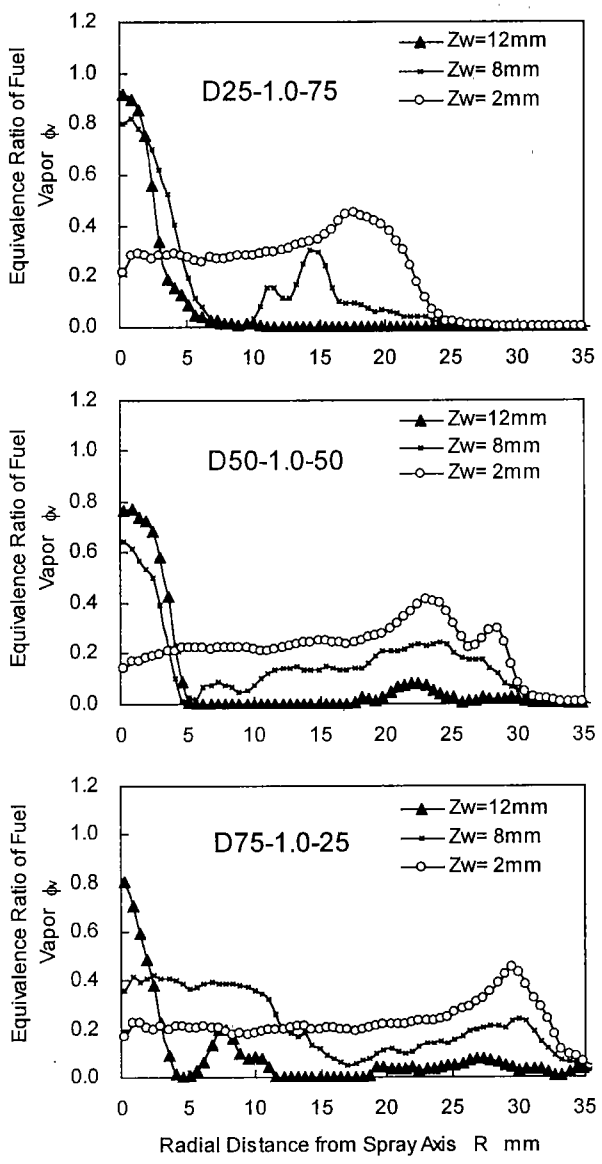

Fig. 9 Radial distributions of equivalence ratios of vapor in split-injection diesel sprays (at the start of the second injection)

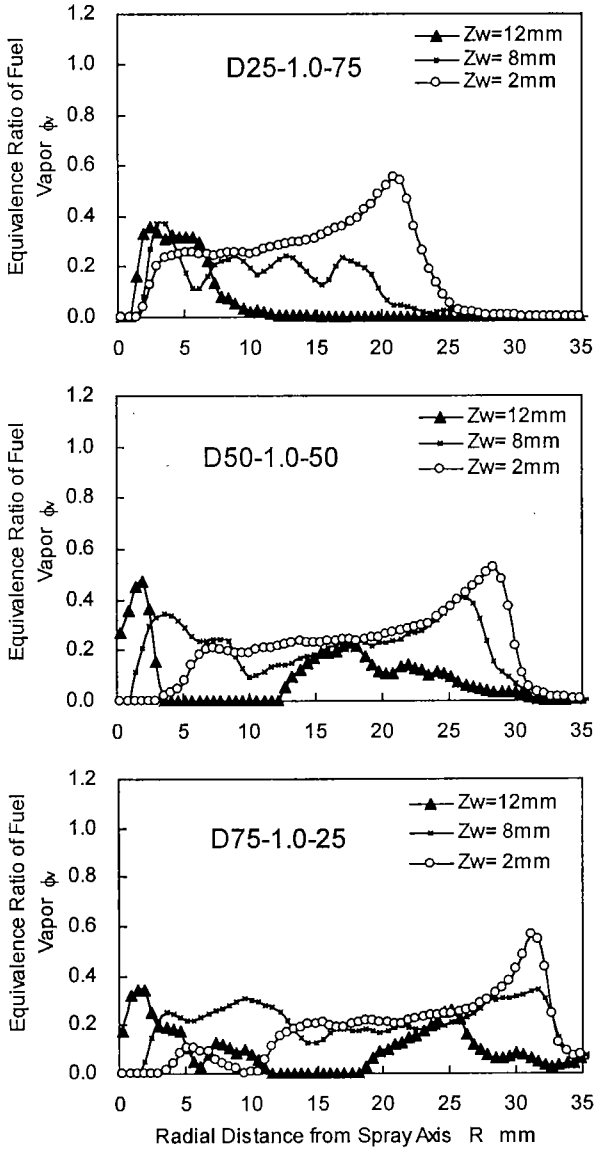

Fig. 10 Radial distributions of equivalence ratios of vapor in split-injection diesel sprays (at about 0.5ms after the second injection starts)

Ltd. by providing the fuel injection system. Special thanks are also due to Mr. T. Ito and Mr. K. Shirotori for their assistance in experiments and data processing.

References

(1) Tow, T., Pierpont, A., and Reitz, R. D., SAE Paper 940897 (1994) , pp.1-15.
(2) Nehmer, D. A., and Reitz, R. D., SAE Paper 940668 (1994), pp.1-12.
(3) Pierpont, D. A., Montgomery, D. T. and Reitz, R. D., SAE Paper 950217 (1995), pp.1-12.
(4) Zhang, Y., Ph.D. Dissertation, University of Hiroshima (2001), pp.59-68.
(5) L. A. Melton, and J. F. Verdieck, 20th Symposium (International) on Combustion, 1283-1290 (1984).
(6) Chraplyvy, Applied Optics, Vol. 20, No. 15, 2620-2624 (1981).
(7) Suzuki, M., Nishida, K. and Hiroyasu, H., SAE Paper 930863 (1993), pp.1-23.
(8) Zhang, Y., Yoshizaki, T. and Nishida, K., Applied Optics, Vol.39, No.33 (2000), pp.6221-6229.
(9) Zhang, Y., Nishida, K. and Yoshizaki, T., SAE Paper 2001-01-1294 (2001), pp.1-12.
(10) Zhang, Y., Ito, T., Yoshizaki, T. and Nishida, K., Transactions of JSAE (Society of Automobile Engineers, Japan), Vol. 32, No. 3 (2001), pp. 37-42.
(11) Zhang, Y., Nishida, K. and Yoshizaki, T., Proceedings of COMODIA 2001, The 5th International Symposium on Diagnostics and Modeling of Combustion (2001), pp. 518-525.
(12) Drallmeier, J. A., Applied Optics, Vol.33, No.30 (1994), pp.7175-7179.
(13) Bohren, E. E. and Huffman, D. R., Absorption and Scattering of Light by Small Particles, Wiley-Interscience, New York (1988), pp.69-81.
(14) Kamimoto, T., Yokota, H. and Kobayashi, H., SAE Paper 890316 (1989), pp1-12.
(15) Mammond, D. C., Jr., Applied Optics, Vol. 20, No.3 (1981), pp. 493-499.
(16) Fujimoto, H., JSME Transactions (B), Vol. 58, No. 552, (1992), pp.2359-2365.
(17) Katsura, N., Saito, M., Senda, J., Fujimoto, H., JSME Transactions (B), Vol. 56, No. 521, (1990), pp. 227-234.